# Mutations on M3 helix of *Plutella xylostella* glutamate-gated chloride channel confer unequal resistance to abamectin by two different mechanisms

Xingliang Wang[a], Alin M. Puinean[b], Andrias O. O´Reilly[c], Martin S. Williamson[b], Charles Smelt[d], Neil S. Millar[d], Yidong Wu[a,*]

[a] College of Plant Protection, Nanjing Agricultural University, Nanjing, China
[b] Rothamsted Research, Biological Chemistry and Crop Protection Department, Harpenden, UK
[c] School of Natural Sciences and Psychology, Liverpool John Moores University, Liverpool, UK
[d] Department of Neuroscience, Physiology and Pharmacology, University College London, London, UK

* Corresponding author.

E-mail addresses:
wxl@njau.edu.cn (X. Wang)
mirel.puinean@rothamsted.ac.uk (A. M. Puinean)
A.O.OReilly@ljmu.ac.uk (A. O. O'Reilly)
martin.williamson@rothamsted.ac.uk (M. S. Williamson)
charles.smelt.13@ucl.ac.uk (C. Smelt)
n.millar@ucl.ac.uk (N. S. Millar)
wyd@njau.edu.cn (Y. Wu)

**Abstract**

Abamectin is one of the most widely used avermectins for agricultural pests control，but the emergence of resistance around the world is proving a major threat to its sustained application. Abamectin, acts by direct activating glutamate-gated chloride channels (GluCls) and modulating other Cys-loop ion channels. To date, three mutations occurring in the transmembrane domain of arthropod GluCls are associated with target-site resistance to abamectin: A309V in *Plutella xylostella* GluCl (PxGluCl), G323D in *Tetranychus urticae* GluCl1 (TuGluCl1) and G326E in TuGluCl3. To compare the effects of these mutations in a single system, A309V/I/G and G315E (corresponding to G323 in TuGluCl1 and G326 in TuGluCl3) substitutions were introduced individually into the PxGluCl channel. Functional analysis using *Xenopus* oocytes showed that the A309V and G315E mutations reduced the sensitivity to abamectin by 4.8- and 493-fold, respectively. In contrast, substitutions A309I/G show no significant effects on the response to abamectin. Interestingly, the A309I substitution increased the channel sensitivity to glutamate by one order of magnitude (*c.a.*12-fold). Analysis of PxGluCl homology models indicates that the G315E mutation interferes with abamectin binding through a steric hindrance mechanism. In contrast the structural consequences of the A309 mutations are not so clear and an allosteric modification of the binding site is the most likely mechanism. Overall the results show that both A309V and G315E mutations may contribute to target-site resistance to abamectin, and could impact future prediction and monitoring of abamectin resistance in *P. xylostella* and other arthropod pests.

**Keywords:** Abamectin, Glutamate-gated chloride channel, Target-site resistance, Molecular modelling

## 1. Introduction

Avermectins are naturally occurring 16-membered macrocyclic lactones produced by fermentation of the soil-dwelling microorganism *Streptomyces avermitilis*. These compounds have potent activity against many kinds of endoparasitic nematodes and ectoparasitic arthropods (Campbell, 2012). Since their first isolation in the 1970's, they have been applied globally for crop protection and animal health purposes. Among the avermectin family members, abamectin (avermectin $B_1$) is one of the most widely used compounds for agricultural pest management (Clark et al., 1995), and ivermectin (a synthetic derivative of avermectin $B_1$, IVE) is active at extremely low dosage against a range of nematode and arthropod parasites (Campbell et al., 1983). Avermectins are classified as neurotoxins, which act by directly activating or potentiating glutamate-gated chloride channels (GluCls) (and to a lesser extent γ-amino butyric acid (GABA)-gated chloride channels). GluCls contribute extensively to invertebrate nervous system function, including modulating locomotion, regulating feeding and mediating sensory inputs (Wolstenholme, 2012) and so modification of channel function by avermectins action can result in paralysis and death (Bloomquist, 1996, 2003).

GluCls belong to the Cys-loop superfamily of ligand-gated ion channels that assemble as pentamers to form a central ion-conducting pore; these GluCl receptors are present only in invertebrates (Jones and Sattelle, 2008; Wolstenholme, 2012). GluCls were first described in electrophysiological studies on locust muscle, when a biphasic change in its membrane potential was recorded and glutamate-enhanced chloride permeability resulted in the hyperpolarizing phase (Cull-Candy, 1976). The first cloned genes encoding GluCl subunits were glucl-α and glucl-β (now referred to *glc-1* and *glc-2*, respectively) from the nematode *Caenorhabditis elegans*. When expressed in *Xenopus* oocytes GluCls composed of glucl-α subunits were response to IVE but not to L-glutamate whereas conversely homomeric glucl-β channels were unresponsive to IVE but were activated by L-glutamate (Cully et al., 1994; Daeffler et al., 2014). The co-expression of both α and β subunits produced channels that robustly responded to both glutamate and IVE independently and so more closed resembled the naturally-occurring receptor (Cully et al., 1994; Vassilatis et al., 1997; Slimko et al., 2002;

Degani-Katzav et al., 2016). The *C. elegans* GluCl gene family has since been expanded to six members (Jones and Sattelle, 2008). Genomic analysis has shown that a single GluCl gene, with variant transcripts produced by mRNA splicing and extensive editing, is present in several insects, including *Drosophila melanogaster, Apis mellifera, Nasonia vitripennis,* and *Tribolium castaneum* (Semenov and Pak, 1999; Jones and Sattelle, 2006, 2007; Jones et al., 2010; Knipple and Soderlund, 2010). Multiple GluCl genes have been identified in other organisms: two in *Aplysia californica,* six in *Tetranychusur ticae* and one in *Lepeophtheirus salmonis* (Tribble et al., 2007; Kehoe et al., 2009; Dermauw et al., 2012).

Several experiments based on functional analysis of IVE-resistant GluCl channels in nematodes predicted that IVE acts by insertion between transmembrane domain of GluCls (Dent et al., 2000; Njue et al., 2004). Recently, our knowledge of the structural and functional properties of the GluCls has made a greatly enrich attribute to development of the three-dimensional crystallographic structure of *C. elegans* GluClα channel (CeGluClα), which presented the first high-resolution view of a eukaryotic Cys-loop receptor (Hibbs and Gouaux, 2011). This X-ray structure revealed that GluCls are arranged with five-fold symmetry and the transmembrane M2 helices form the pore lumen. The pore-lining residues of the M2 helices therefore determine the ion selectivity and conductance properties of the channel (Hibbs and Gouaux, 2011). This structure was co-crystallized with IVE, which binds in the transmembrane domain at subunit interfaces, lying between M3 and M1 helices of two adjacent subunits and making binding contacts with M2 and the M2-M3 loop. The endogenous ligand glutamate binds in the extracellular domain of the receptor in the classical neurotransmitter position, which is also located at the interface of adjacent subunits.

The diamondback moth, *Plutella xylostella,* is one of the few insect species that has evolved field resistance to all primary classes of insecticides (Furlong et al., 2013). As such it represents a valuable agricultural pest model to study the genetics and mechanisms of resistance development (Furlong et al., 2013). Gene mutations mediated resistance mechanism has been widely studied in *P. xylostella*, occurred in acetylcholinesterase, sodium channel, nicotinic acetylcholine receptor, GluCl, ryanodine receptor and ABC transporter C2, which involved in resistance to organophosphorous, pyrethroid, spinosad, abamectin,

chlorantraniliprle, Bt Cry1Ac toxin, indoxacarb and metaflumizone, respectively (Schuler et al., 1998; Lee et al., 2007; Baxter et al., 2010, 2011; Troczka et al., 2012; Guo et al., 2014; Wang et al., 2016a, 2016b, 2016c). Abamectin has been used for *P. xylostella* control since the 1980's and at least 72 cases from four countries have been reported of field resistance to this chemical (APRD, 2017). A detailed study of the molecular mechanisms of abamectin resistance is important for designing strategies to circumvent it. In our previous work, a combination of genetics and sequencing identified a point mutation (A309V) in the transmembrane domain of *P. xylostella* glutamate-gated chloride channel receptor, PxGluCl, which has been evaluated to contribute *c.a.* 10-fold increase to abamectin resistance in the resistant Roth-Abm strain (Wang et al., 2016b). We believe that characterizing the pharmacological properties of this mutation that evolved in PxGluCl could help in exploring the resistance mechanisms in this and other species and might inform the development of new macrocyclic lactones insecticides.

In addition to A309V, only three other mutations in GluCls have been reported in association with resistance to avermectins (IVE & abamectin) in other arthropods (Fig. 1). The P299S mutation of the *D. melanogaster* DmGluCl channel is associated with a 3-fold resistance to IVE in this insect (Kane et al., 2000). The TuGluCl1 G323D and TuGluCl3 G326E mutations are associated with 18- and 2000-fold resistance to abamectin in *T. urticae*, respectively (Kown et al., 2010; Dermauw et al., 2012). Of these only the P299S mutation has been characterized electrophysiologically and a 14-fold reduction in IVE sensitivity was found when this substitution was introduced into DmGluCl (Kane et al., 2000). In the current study, we expressed A309V or G315E (equivalent to G323 in TuGluCl-1 and G326 in TuGluCl-3) mutants of PxGluCl in *Xenopus laevis* oocytes and compared their functional properties with wild-type receptors. Also, further mutations of A309 to glycine or isoleucine were generated to investigate how substitutions at this position on the M3 helix could affect glutamate or abamectin binding. Homology models were generated to provide structural insight into the molecular mechanisms that underlie the abamectin resistance of these mutations.

## 2. Materials and methods

*2.1. Chemicals and reagents*

L-Glutamic acid (≧99%) and abamectin ($B_1a$ = 91.5%), used for two-electrode voltage-clamp recording, were purchased from Sigma-Aldrich (St. Louis, MO, USA) and Veyong bio-chemical (Shijiazhuang, Hebei, China), respectively. All the restricted enzymes used in this study, including *Eco*RI, *Xba*I, *Sma*I, *Not*I and the klenow fragment were purchased from Thermo Fisher Scientific (Waltham, MA, USA).

*2.2. Site-directed mutagenesis and cRNA synthesis*

Total RNA of 4$^{th}$-instar larvae from *P. xylostella* susceptible Roth strain was extracted by using the SV Total RNA Isolation System Kit (Promega, Madison, WI, USA) according to the manufacturer's protocol. First-strand cDNA was synthesized from 1 μg total RNA using an oligo(dT)$_{15}$ primer and M-MLV reverse transcriptase (Promega, Madison, WI, USA). The full-length cDNA of wild-type PxGluCl (GenBank accession no. JX014231.1) was amplified by PrimeSTAR HS DNA polymerase (TaKaRa, Japan) and PCR (35 cycles of 98 °C for 10 s, 53 °C for 15s, and 72 °C for 90 s) with the forward primer PxGluCl_*Eco*RⅠ_F and the corresponding reverse primer PxGluCl_*Xba*Ⅰ_R (Table 1). Site-directed mutagenesis was performed by fusion PCR with wild-type PxGluCl cDNA as the template. All the cDNA constructs were ligated into the pEASY-Blunt Cloning vector (Beijing TransGen Biotech Co. Ltd, Beijing, China) and the isolated plasmid DNAs were examined by nucleotide sequencing (Life Technology, Shanghai, China). Five full-length *P. xylostella* GluCl cDNA (wild-type, A309V, A309I, A309G and G315E) were subcloned into the pGH19 vector, a modified version of plasmid pGEMHE，which contains 5′- and 3′-untranslated *X. laevis beta*-globin gene regions, and the presence of the mutations/substitutes were reconfirmed by sequencing. Plasmids were linearized with *Not*I, and capped RNAs were carried out using the T7 mMessage mMachine Kit (Ambion, Life Technologies, Paisley, UK) according to the manufacturer's instruction. Synthesized cRNAs were recovered by precipitation with isopropanol, dissolved in nuclease-free water at a final concentration of 500 ng/μL and stored at -80 °C until use.

*2.3. Functional expressions of* PxGluCl *variants in* X. laevis *oocytes*

Mature healthy *X. laevis* oocytes (stage V–VI) were treated with collagenase (type IA; 2 mg/ml; Sigma, USA) in calcium-free Barth's solution (88 mM NaCl, 2.4 mM $NaHCO_3$,15 mM Tris-HCl, 1 mM KCl and 0.82 mM $MgCl_2$) for about 25 min at room temperature, rinsed three times, and manually defolliculated before injection with cRNA. Oocytes were injected with 5-15 ng cRNA in a volume of 32.2 nL into the cytoplasm by using a Drummond variable volume microinjector. After injection, calcium-containing Barth's solution (0.77 mM) with antibiotics (100 units/mL penicillin, 100 μg/mL streptomycin, 4 μg/mL kanamycin and 50 μg/mL tetracycline) was used for oocytes' incubation at 18 °C. Experiments were carried out at room temperature between 3 and 5 days after injection.

### *2.4. Two-electrode voltage clamp electrophysiology*

Two-electrode voltage clamp was used for recording whole-cell currents from the injected *Xenopus* oocytes. The oocytes were held in a recording bath and continuously perfused with a Ringer's solution (115 mM NaCl, 2.5 mM KCl, 1.8 mM $CaCl_2$ and 10 mM Hepes, pH 7.3). The glass capillary electrodes were filled with 3M KCl and have a resistance of 0.5-1.5 MΩ. Glutamate and abamectin induced inward currents were recorded with an OC-725C oocyte clamp (Warner Instruments, Hamden, CT, USA) at a holding potential of -60 mV. Data acquisition and analysis were carried out using iWorx 408 data acquisition system and LabScribe software (iWorx Systems, Inc. Dover, NH, USA). Glutamate was dissolved in Ringer's solution and applied to the oocytes for 3 s. After the glutamate perfusion, the oocytes were washed by Ringer's solution for 2 min to assess their reproducibility. Abamectin was first dissolved in DMSO (0.1 mM) and then diluted with Ringer's solution. The abamectin solution containing ≤ 0.1% DMSO was applied to oocytes for 15 s, and the oocytes were then washed for 3.5 min. Because of the effects of abamectin was irreversible, activated currents were normalized to the saturating glutamate-induced current in the same oocyte. Dose-response data were analyzed by nonlinear regression analysis using GraphPad Prism 5.0 (GraphPad Software Inc., San Diego, CA, USA). Data were obtained for at least four oocytes from at least two frogs, and the values are given as means ± SEM. Statistical analysis was determined by a two-tail Student's *t*-test.

### *2.5. Homology modeling of* PxGluCl *mutants*

An homology model of the open-state *P. xylostella* glutamate-gated chloride channel (GenBank accession no. JX014231.1) was generated as described (Wang et al., 2016b). A docking prediction of avermectin B1a with the open-state *P. xylostella* open-state model was also previously generated (Wang et al., 2016b). In this study, mutations were introduced into the channel model using Swiss-PdbViewer software (Guex et al., 1999) followed by 30 steps of steepest descent then 50 steps of conjugate gradient energy minimization. Figures were produced using PyMOL (DeLano Scientific, San Carlos, CA, USA).

### *2.6. Genomic DNA extraction and mutations screening of* PxGluCl *in field populations*

To determine whether the A309V and G315E mutations of PxGluCl have evolved in field population of *P. xylostella,* PCR amplification was carried out with genomic DNA isolated from individual larvae using the AxyPrep™Multisource Genomic DNA Miniprep Kit (Axygen Biosciences, Union, CA, USA) according to the manufacturer's protocol. A genomic DNA fragment of PxGluCl, covering the M3 region, was amplified as described previously (Wang et al., 2016b). 20-40 samples from seventeen *P. xylostella* populations collected in China during 2013-2015 were successful examined by direct nucleotide sequencing using a gene-specific primer (Wang et al., 2016b). The genotypes of 309 and 315 positions of the PxGluCl were identified according to sequence chromatograms.

## 3. Results

### *3.1. Response of wild-type and mutant channels to glutamate*

We cloned the full-length cDNA sequence of wild-type PxGluCl (the most common isoform 3c9a) from the susceptible Roth strain. The natural-occurring mutations PxGluCl-A309V (found in *P. xylostella* by Wang et al., 2016b) and PxGluCl-G315E (equivalent to G326E mutation found in *T. urticae* by Dermauw et al., 2012) were then introduced and two other mutants (PxGluCl-A309I, PxGluCl-A309G) were generated (Table 1 and Fig. 1). The application of glutamate to these five channels induced robust inward currents in a dose-dependent fashion (Fig. 2). The dose-response curves gave $EC_{50}$s of 19.93 ± 3.26 μM, 13.24 ± 1.05μM, 1.67 ± 0.20μM，34.60 ± 2.83μM and 10.35 ± 3.67μM for wild-type, A309V, A309I, A309G and G315E channels, respectively, and they produced nHs

of 1.75 ± 0.18, 0.98 ± 0.06, 2.47 ± 0.31,0.70 ± 0.05 and 1.03 ± 0.09 for wild-type, A309V, A309I, A309G and G315E channels, respectively (Table 2). The A309V and G315E increased the potency of glutamate by 1.5- and 1.9-fold, respectively, without significant differences observed in $EC_{50}$s when compared with the wild-type channel.

Interestingly, the A309I mutant exhibited an approximately 12-fold increase in glutamate sensitivity (Fig. 2B), and the difference of $EC_{50}$s and nHs between A309I and wild-type channel were significant ($p < 0.05$). In contrast, the A309G mutant was less sensitive to glutamate, with a 1.7-fold reduction compared with wild-type. The Hill coefficient for the A309I and A309G mutants was 2.5 and 0.7, respectively, which suggests that the number of occupiable glutamate-binding sites in these receptors changed compared to wild-type.

*3.2. Response of wild-type and mutant channels to abamectin*

Unlike the glutamate response, application of abamectin induced slow-to-activate and irreversible currents (Fig. 3A), and it was observed in all channels in a dose-dependent manner (Fig. 3B). The current did return to original baseline even after washing for several minutes with Ringer's solution. The $EC_{50}$s of abamectin calculated from the dose-response relationships of wild-type, A309V, A309I, A309G and G315E channels were 0.16 ± 0.05μM, 0.78 ± 0.02 μM, 0.25 ± 0.01μM, 0.15 ± 0.02 μM and 80.32 ± 23.67 μM, respectively (Table 2). The results showed that the curve for abamectin was right-shifted in A309V (Fig. 3B), and the $EC_{50}$ reduced 5.0-fold but significantly ($p = 0.0284$), when compared with that of the wild-type. However, both of the A309I and A309G mutated channels had similar $EC_{50}$ values ($p > 0.05$) to that wild-type channel (Table 2 and Fig. 3B).

In contrast, the G315E channel showed greatly reduced sensitivity to abamectin, yielding a 493-fold right-shift of $EC_{50}$ compared with that of wild-type (Table 2 and Fig. 3B), and the observed reduction of $EC_{50}$ between G315E and wild-type channel were significantly different ($p = 0.0173$). Especially, the response of G315E channel to the highest concentration of abamectin used in this study (0.3 mM), reached only 63 ± 4.1% of the response to saturating glutamate-activated current (0.1 mM). It is therefore predicted that the G315E mutation in PxGluCl may abolish abamectin potency.

### *3.3. Molecular models of* PxGluCl *mutants*

A model of PxGluCl in the open state and in complex with abamectin was previously generated (Wang et al., 2016b) using the crystal structure of CeGluClα in complex with IVE (Hibbs and Gouaux, 2011) as the homology template. As found previously with the A309V mutation, there were no steric clashes encountered when A309 was substituted with either glycine or isoleucine (Fig. 4). Furthermore, even introduction of the larger isoleucine side-chain did not result in novel binding contacts forming with abamectin. This is due to the register of the M3 helix whereby the 309 side chain is orientated away from the insecticide binding site (Fig. 4).

G315 is also located on M3 but, in contrast to A309, the side chain of this residue is orientated towards the ligand binding domain (Fig. 5). This glycine is predicted to form van der Waals interactions with abamectin, which is also found with IVE and the conserved M3 glycine in the open-state CeGluClα structure (Hibbs and Gouaux, 2011). The effect of the G315E mutation was to produce a major steric clash with the benzofuran moiety of abamectin (Fig. 5).

### *3.4. Mutation screening in field populations*

As has been described in Wang et al. (2016b), we have established a rapid detection method for the mutation occurred in M3 by using the direct-sequencing chromatograph. The A309V mutation was first identified in Roth-Abm, which was obtained from a field population TH with high-level of abamectin resistance (Pu et al., 2010), indicating that A309V was present in the field. Both TH13 and TH16 were also collected in 2013 and 2016 from Tonghai County, Yunnan Province, China. Genotype detection has revealed that TH16 population consisted of 16 homozygous wild-type (Ala at position 309) and 4 heterozygous (Ala/Val) individuals, and the mutant frequency reached to 10% (Table 3). TH13 population collected 2yrs ago had also been detected carrying 6.25% mutant alleles. By contrast, five populations from Southeast China, which evolved high levels of resistance to abamectin (49- to 253-fold, unpublished data), but the A309V mutation was not detected in these populations. However, 2 of 8 populations (KS14 and KS15) from Eastern China have been detected

carrying 3.33% and 1.67% mutant alleles, respectively, although both of them had low levels of resistance to abamectin. In general, heterozygous and homozygous mutant-type individuals with the A309V mutation have been detected in field populations collected from China, but the reported mutations (G323D and G326E in TuGluCls) equivalent to G315 position of PxGluCl have not been screened in the 17 field populations.

## 4. Discussion

In this study we cloned and functionally expressed PxGluCl from an abamectin-susceptible strain of *P. xylostella*. The function and pharmacology of mutations relevant to abamectin resistance were also characterized. In addition, populations of abamectin-resistant *P. xylostella* were genotyped to detect the occurrence of mutations at the A309 or G315 positions in the field. We previously demonstrated that the A309V mutation of PxGluCl was strongly associated with a 10-fold increase in abamectin resistance in *P. xylostella* Roth-Abm strain (Wang et al., 2016b). Here we show by expressing the wild-type or A309V channels in oocytes that the mutant exhibits a modest but significant (*c.a.*5-fold) reduction of abamectin sensitivity relative to the wild-type channel. This finding strongly suggests that target-site resistance indeed plays a role in abamectin resistance of *P. xylostella* pest populations in the field.

We hypothesized that A309V may confer resistance by allosterically modifying the abamectin binding site (Wang et al., 2016b). To investigate this further the A309G and A309I mutants were generated, as these residues have side chains that are either smaller or bigger than wild-type or A309V. The A309G mutation showed equivalent abamectin sensitivity compared with wild-type whereas the A309I channel showed a 1.5-fold decrease in abamectin sensitivity, which contrasts with the 5-fold resistance exhibited by A309V. Modelling of the receptor shows, as with A309V (Wang et al., 2016b), the A309G and even the larger A309I side chain can be accommodated without sterically perturbing the structure (Fig. 4). In addition, substitutions at the 309 position are still too far from the abamectin binding site to interact directly with the ligand, further supporting the hypothesis of an allosteric mechanism underlying resistance.

Intriguingly, A309 substitutions also affected glutamate sensitivity. A 1.7-fold reduction of glutamate sensitivity was detected with A309G, a 1.5-fold increase in sensitivity with A309V and surprisingly the A309I had increased glutamate sensitivity by one order of magnitude (12-fold). The 309 position is located on the top of the M3 helix and so distal from the glutamate binding site (see Fig. 6A in Wang et al., 2016b). Nevertheless, it is contiguous with the M2-M3 linker, which is critical for transmitting neurotransmitter-induced conformational changes in the extracellular domain to the transmembrane domain to gate the pore (Althoff et al., 2014). Degani-Katzav et al. (2016) identified a mutation in the IVE-binding site of M1 (αL279W; equivalent to α(-)L218 of CeGluCl crystal structure) that reduced the $EC_{50}$ of glutamate by about 25-fold, when compared with the *C. elegans* wild type receptor. Similarly, Daeffler et al. (2014) introduced several mutant amino acids of varying size and polarity in to the M2 helix of *C. elegans* GluClβ receptor, four of these mutations led to 9- to 44-fold increase in channel sensitivity to glutamate, respectively. In the current study, it appears that larger residues at the top of M3 of PxGluCl facilitate channel opening, although the model reveals that the replacement of the alanine side chain with the larger isoleucine side chain didn't produce any steric clashes. Further studies will be required to determine why the A309I mutant is more sensitive to glutamate and to explain why the Hill coefficient has increased from 1.8 to 2.5, which suggests the presence of an additional glutamate binding site. Yet the effect of the A309I mutation clearly demonstrates the influence of this 309 position on GluCl pharmacology.

In the case of the A309V receptor, it is possible that this mutation does not allosterically modify the binding site for abamectin, thus inhibiting its binding. Instead this mutation may allosterically counteract the functional effect of the insecticide upon binding. We attempted to investigate this by quantifying binding affinity using radioligand binding studies of [$^3$H]-avermectin to membranes of the PxGluCls expressed in *Drosophila* S2 cell lines. Unfortunately these studies were not successful, due to extremely high levels of nonspecific binding of [$^3$H]-avermectin to membranes (data not shown). This is almost certainly due to the very lipophilic nature of the radioligand. A similar predicament was encountered when investigating the binding sites of pyrethroids on insect sodium channels (Rossignol, 1988;

Pauron et al., 1989; Dong and Scott, 1994).

The current work also represents the first effort to characterize the pharmacological effect of naturally occurring G315E mutation. This mutation is tightly linked to abamectin resistance in the MAR-AB strain of *T. urticae*, with a resistance level of more than 2000-fold (Dermauw et al., 2012). The equivalent G323D mutation is associated with a 18-fold resistance to abamectinin an isogenic-resistant strain (Kwon et al., 2010). Our electrophysiology findings show that introducing the G315E mutation into PxGluCl resulted in 493-fold resistance to abamectin. Glycine is entirely conserved in M3 helix of GluCls and the role of substitutions at this"M3-Gly" position in conferring resistance to avermect in compounds has been well characterized (Lynagh and Lynch, 2012). Human glycine receptor α1 receptor (GlyRα1) has an alanine at the equivalent position and showed that IVE-sensitivity (50-fold) can be conferred on an IVE-insensitive receptor by introducing a M3-Gly at this position. Furthermore, the reciprocal introduction in the *Haemonchus contortus* α3BGluCl, G329A (the human GlyRα1 equivalent posotion) shifts the $EC_{50}$ of IVE activation from 39 nM up to 1200 μM. This indicates that M3-Gly is essential for high IVE sensitivity in both glycine- and glutamate- gated Cys-loop receptors (Lynagh and Lynch, 2010). The proposed resistance mechanism for M3-Gly mutations (Lynagh and Lynch, 2012) is that a larger side chain at this position sterically obstructs entry of an avermectin ligand to the narrow gap between the M3 helix of principal subunit and M1 of the complementary subunit and thus limits access to the insecticide binding site.

Recently, resistance to abamectin began to emerge and develop in field populations of various arthropod pests in worldwide, including twenty-one species form Lepidoperan, Acari, Blattodea, Coleoptera, Diptera, Hemiptera, Mesostigmata and Thysanoptera (APRD, 2017). Without doubt, identification of abamectin-resistant mutations will be very valuable for elucidating the molecular mechanisms and monitoring the development of resistance to abamectin. In this work, in total 503 larvae sampled from 17 field *P. xylostella* populations were analyzed for the estimation of the frequency of the A309V and G315D/E mutations, previously associated with abamectin resistance in arthropods. The A309V mutation was detected in four populations with lower frequencies. Two populations collected from Tonghai

county in 2013 and 2016 (TH13, TH16), where abamectin was mainly employed in the control of *P. xylostella* and control failure always reported by local farmers, showed 6.25% and 10% mutant allele frequencies. In contrast, G315D/E has not been detected in any tested populations from China. Resistance development of field populations is complex, and resistant phenotype might be associated with metabolic detoxification of abamectin and other potential mechanisms. Although insecticide resistance development may or may not result in control failure, it has given rise to the loss of many selective compounds that could otherwise have formed part of insecticide resistance management (IRM) and, more broadly, integrated pest management programs for *P. xylostella*. In view of the A309V mutation detected in *P. xylostella* field populations, and the G314D and G326E mutations have been reported in *T. urticae*, originating from rose greenhouses with varied frequencies (from 5% to 100%) (Ilias et al., 2016), molecular diagnostic assays for early identification and monitoring of low-frequency A309V and G315D/E allelles of PxGluCl in a globally collected samples is required in IRM strategies of *P. xylostella*.

In conclusion, here we functionally characterized the potency of abamectin and the endogenous neurotransmitter glutamate on the activity of wild-type and mutant PxGluCls. Two naturally occurring mutations in the M3 helix of arthropod GluCls that are associated with abamectin resistance reduced the channel sensitivity to this compound. We suggest that two different mechanisms are involved in abamectin target-site resistance, with the G315 mutation directly sterically hindering abamectin binding while the A309V mutation possibly allosterically modifies the ligand binding site. Fitness analysis is required to define the physiological function and/or negative effects of these mutations on insects. Our study provide direct evidences that A309V and G315E mutations on M3 helix can results in abamectin resistance, and we also suggest that resistant alleles should be monitored continuously, which will provide useful information for investigating the evolution and spread of well-characterized resistance genes.

**Acknowledgements**

This work was supported by grants from National Natural Science Foundation of China (31301693), the Chinese Ministry of Agricultural 948 project (2014-S10) and the National

Key Research and Development Program of China (2016YFD0200500).

## References

Althoff, T., Hibbs, R.E., Banerjee, S., Gouaux, E., 2014. X-ray structures of GluCl in apo states reveal a gating mechanism of Cys-loop receptors. Nature 512, 333-337.

APRD, 2017. Arthropod pesticide resistance database.http://www.pesticideresistance.com/. Accessed on 15, Mar. 2017.

Baxter, S.W., Badenes-Perez, F.R., Morrison, A., Vogel, H., Crickmore, N., Kain, W., Wang, P., Heckel, D.G., Jiggins, C.D., 2011. Parallel evolution of *Bacillus thuringiensis* toxin resistance in Lepidoptera. Genetics 189, 675-679.

Baxter, S.W., Chen, M., Dawson, A., Zhao, J.Z., Vogel, H., Shelton, A.M., Heckel, D.G., Jiggins, C.D., 2010. Mis-spliced transcripts of nicotinic acetylcholine receptor alpha 6 are associated with field evolved spinosad resistance in *Plutella xylostella* (L.). PLoS Genet. 6, e1000802.

Bloomquist, J.R., 1996. Ion channels as targets for insecticides. Annu. Rev. Entomol. 41, 163-190.

Bloomquist, J.R., 2003. Chloride channels as tools for developing selective insecticides. Arch. Insect Biochem. Physiol. 54, 145-156.

Campbell, W.C., 2012. History of avermectin and ivermectin, with notes on the history of other macrocyclic lactone antiparasitic agents. Curr. Pharm. Biotechnol. 13, 853-865.

Campbell, W.C., Fisher, M.H., Stapley, E.O., Albers-Schonberg, G., Jacob, T.A., 1983. Ivermectin: a potent new antiparasitic agent. Science 221, 823-828.

Clark, J.M., Scott, J.G., Campos, F., Bloomquist, J.R., 1995. Resistance to avermectins-extent, mechanisms, and management implications. Annu. Rev. Entomol. 40, 1-30.

Cull-Candy, S.G., 1976. Two types of extrajunctional L-glutamate receptors in locust muscle fibres. J. Physiol. 255, 449-464.

Cully, D.F., Vassilatis, D.K., Liu, K.K., Paress, P.S., Vanderploeg, L.H.T., Schaeffer, J.M., Arena, J.P., 1994. Cloning of an avermectin-sensitive glutamate-gated chloride channel from *Caenorhabditis elegans*. Nature 371, 707-711.

Daeffler, K.N.M., Lester, H.A., Dougherty, D.A., 2014. Functional evaluation of key interactions evident in the structure of the eukaryotic Cys-loop receptor GluCl. ACS. Chemical Biology 9, 2283-2290.

Degani-Katzav, N., Gortler, R., Gorodetzki, L., Paas, Y., 2016. Subunit stoichiometry and arrangement in a heteromeric glutamate-gated chloride channel. Proc. Natl. Acad. Sci. U. S. A. 113, E644-E653.

Dent, J.A., Smith, M.M., Vassilatis, D.K., Avery, L., 2000. The genetics of ivermectin resistance in *Caenorhabditis elegans*. Proc. Natl. Acad. Sci. U. S. A. 97, 2674-2679.

Dermauw, W., Ilias, A., Riga, M., Tsagkarakou, A., Grbic, M., Tirry, L., Van Leeuwen, T., Vontas, J., 2012. The cys-loop ligand-gated ion channel gene family of *Tetranychus urticae*: implications for acaricide toxicology and a novel mutation associated with abamectin resistance. Insect Biochem. Mol. Biol. 42, 455-465.

Dong, K., Scott, J.G., 1994. Linkage of *kdr*-type resistance and the *para*-homologous sodium-channel gene in German Cockroaches (*Blattella germanica*). Insect Biochem. Mol. Biol. 24, 647-654.

Furlong, M.J., Wright, D.J., Dosdall, L.M., 2013. Diamondback moth ecology and management: problems, progress, and prospects. Annu. Rev. Entomol. 58, 517-541.

Guex, N., Diemand, A., Peitsch, M.C., 1999. Protein modelling for all. Trends. Biochem. Sci. 24, 364-367.

Guo, L., Liang, P., Zhou, X.G., Gao, X.W., 2014. Novel mutations and mutation combinations of ryanodine receptor in a chlorantraniliprole resistant population of *Plutella xylostella* (L.). Sci. Rep. 4, 6924.

Hibbs, R.E., Gouaux, E., 2011. Principles of activation and permeation in an anion-selective Cys-loop receptor. Nature 474, 54-60.

Ilias, A., Vassiliou, V.A., Vontas, J., Tsagkarakou, A., 2017. Molecular diagnostics for detecting pyrethroid and abamectin resistance mutations in *Tetranychus urticae*. Pestic. Biochem. Physiol. 135, 9-14.

Jones, A.K., Bera, A.N., Lees, K., Sattelle, D.B., 2010. The cys-loop ligand-gated ion channel gene superfamily of the parasitoid wasp, *Nasonia vitripennis*. Heredity 104, 247-259.

Jones, A.K., Sattelle, D.B., 2006. The cys-loop ligand-gated ion channel superfamily of the honeybee, *Apis mellifera*. Invert. Neurosci. 6, 123-132.

Jones, A.K., Sattelle, D.B., 2007. The cys-loop ligand-gated ion channel gene superfamily of the red flour beetle, *Tribolium castaneum*. BMC Genom. 8, 327

Jones, A.K., Sattelle, D.B., 2008. The cys-loop ligand-gated ion channel gene superfamily of the nematode, *Caenorhabditis elegans*. Invert. Neurosci. 8, 41-47.

Kane, N.S., Hirschberg, B., Qian, S., Hunt, D., Thomas, B., Brochu, R., Ludmerer, S.W., Zheng, Y., Smith, M., Arena, J.P., Cohen, C.J., Schmatz, D., Warmke, J., Cully, D.F., 2000. Drug-resistant *Drosophila* indicate glutamate-gated chloride channels are targets for the antiparasitics nodulisporic acid and ivermectin. Proc. Natl. Acad. Sci. U. S. A. 97, 13949-13954.

Kehoe, J., Buldakova, S., Acher, F., Dent, J., Bregestovski, P., Bradley, J., 2009. Aplysia cys-loop glutamate-gated chloride channels reveal convergent evolution of ligand specificity. J. Mol. Evo. 69, 125-141.

Knipple, D.C., Soderlund, D.M., 2010. The ligand-gated chloride channel gene family of *Drosophila melanogaster.* Pestic. Biochem. Physiol. 97, 140-148.

Kwon, D.H., Yoon, K.S., Clark, J.M., Lee, S.H., 2010. A point mutation in a glutamate-gated chloride channel confers abamectin resistance in the two-spotted spider mite, *Tetranychus urticae* Koch. Insect Mol. Biol. 19, 583-591.

Lee, D.W., Choi, J.Y., Kim, W.T., Je, Y.H., Song, J.T., Chung, B.K., Boo, K.S., Koh, Y.H., 2007. Mutations of acetylcholinesterase1 contribute to prothiofos-resistance in *Plutella xylostella* (L.). Biochem. Bioph. Res. Commun. 353, 591-597.

Lynagh, T., Lynch, J.W., 2010. A glycine residue essential for high ivermectin sensitivity in Cys-loop ion channel receptors. Int. J. Parasitol. 40, 1477-1481.

Lynagh, T., Lynch, J.W., 2012. Ivermectin binding sites in human and invertebrate Cys-loop

receptors. Trends. Pharmacol. Sci. 33, 432-441.

Njue, A.I., Hayashi, J., Kinne, L., Feng, X.P., Prichard, R.K., 2004. Mutations in the extracellular domains of glutamate-gated chloride channel alpha 3 and beta subunits from ivermectin-resistant *Cooperia oncophora* affect agonist sensitivity. J. Neurochem. 89, 1137-1147.

Pauron, D., Barhanin, J., Amichot, M., Pralavorio, M., Berge, J.B., Lazdunski, M., 1989. Pyrethroid receptor in the insect Na sup+ channel: alteration of its properties in pyrethroid-resistant flies. Biochemistry 28, 1673-1677.

Pu, X., Yang, Y.H., Wu, S.W., Wu, Y.D., 2010. Characterisation of abamectin resistance in a field-evolved multiresistant population of *Plutella xylostella*. Pest Manag. Sci. 66, 371-378.

Rossignol, D.P., 1988. Reduction in number of nerve membrane sodium channels in pyrethroid resistant house flies. Pestic. Biochem. Physiol. 32, 146-152.

Schuler, T.H., Martinez-Torres, D., Thompson, A.J., Denholm, I., Devonshire, A.L., Duce, I.R., Williamson, M.S., 1998. Toxicological, electrophysiological and molecular characterisation of knockdown resistance to pyrethroid insecticides in the diamondback moth, *Plutella xylostella* (L.). Pestic. Biochem. Physiol. 59, 169-182.

Semenov, E.P., Pak, W.L., 1999. Diversification of *Drosophila* chloride channel gene by multiple posttranscriptional mRNA modifications. J. Neurochem. 72, 66-72.

Slimko, E.M., McKinney, S., Anderson, D.J., Davidson, N., Lester, H.A., 2002. Selective electrical silencing of mammalian neurons in vitro by the use of invertebrate ligand gated chloride channels. J. Neurosci. 22, 7373-7379.

Tribble, N.D., Burka, J.F., Kibenge, F.S.B., 2007. Identification of the genes encoding for putative gamma aminobutyric acid (GABA) and glutamate-gated chloride channel (GluCl) alpha receptor subunits in sea lice (*Lepeophtheirus salmonis*). J. Vet. Pharmacol. Ther. 30, 163-167.

Troczka, B., Zimmer, C.T., Elias, J., Schorn, C., Bass, C., Davies, T.G., Field, L.M., Williamson, M.S., Slater, R., Nauen, R., 2012. Resistance to diamide insecticides in diamondback moth, *Plutella xylostella* (Lepidoptera: Plutellidae) is associated with a mutation in the membrane-spanning domain of the ryanodine receptor. Insect Biochem. Mol. Biol. 42, 873-880.

Vassilatis, D.K., Arena, J.P., Plasterk, R.H.A., Wilkinson, H.A., Schaeffer, J.M., Cully, D.F., van der Ploeg, L.H.T., 1997. Genetic and biochemical evidence for a novel avermectin-sensitive chloride channel in *Caenorhabditis elegans*: isolation and characterization. J. Biol. Chem. 272, 33167-33174.

Wang, J., Wang, X.L., Lansdell, S.J., Zhang, J.H., Millar, N.S., Wu, Y.D., 2016a. A three amino acid deletion in the transmembrane domain of the nicotinic acetylcholine receptor alpha 6 subunit confers high level resistance to spinosad in *Plutella xylostella*. Insect Biochem. Mol. Biol. 71, 29-36.

Wang, X.L., Wang, R., Yang, Y., Wu, S., O'Reilly, A.O., Wu, Y.D., 2016b. A point mutation in the glutamate-gated chloride channel of *Plutella xylostella* is associated with resistance to abamectin. Insect Mol. Biol. 25, 116-125.

Wang, X.L., Su, W., Zhang, J.H., Yang, Y.H., Dong, K., Wu, Y.D., 2016c. Two novel sodium channel mutations associated with resistance to indoxacarb and metaflumizone in the diamondback moth, *Plutella xylostella*. Insect Sci. 23, 50-58.

Wolstenholme, A.J., 2012. Glutamate-gated chloride channels. J Biol. Chem. 287, 40232-40238.

**Table 1**

Sequences of primers used in this study.

| Primer | Use | Sequence (5' to 3') |
|---|---|---|
| PxGluCl_EcoRI_F | Full-length cDNA amplification and fusion PCR | CGGAATTCGGTTTGCTGAGTTGGAGAATGGACG |
| PxGluCl_XbaI_R | Full-length cDNA amplification and fusion PCR | GCTCTAGATGCCAGTGGAACGATGCTGATGC |
| Px_A309V_F | Amplify the downstream fragment of A to V mutation | GTATCATACACAAAGGTCATAGACGTATGGACTGG |
| Px_A309V_R | Amplify the upstream fragment of A to V mutation | CCAGTCCATACGTCTATGACCTTTGTGTATGATAC |
| Px_A309I_F | Amplify the downstream fragment of A to I mutation | GTATCATACACAAAGATCATAGACGTATGGACTGG |
| Px_A309I_R | Amplify the upstream fragment of A to I mutation | CCAGTCCATACGTCTATGATCTTTGTGTATGATAC |
| Px_A309G_F | Amplify the downstream fragment of A to G mutation | GTATCATACACAAAGGGCATAGACGTATGGACTGG |
| Px_A309G_R | Amplify the upstream fragment of A to G mutation | CCAGTCCATACGTCTATGCCCTTTGTGTATGATAC |
| Px_G315E_F | Amplify the downstream fragment of G to E mutation | TAGACGTATGGACTGAGGTTTGTTTAACATTCG |
| Px_G315E_R | Amplify the upstream fragment of G to E mutation | CGAATGTTAAACAAACCTCAGTCCATACGTCTA |

**Table 2**

$EC_{50}$ values and Hill coefficients of L-glutamate- and abamectin-induced responses of PxGluCls expressed in *Xenopus laevis* oocytes. Data were obtained by nonlinear regression analyses and indicated as means and 95% confidence limits (n = 5 ~ 6).

| Variants | L-glutamate (μM) | | | | | Abamectin (μM) | | | | |
|---|---|---|---|---|---|---|---|---|---|---|
| | n | $EC_{50}$ | 95% CL | $n_H$ | 95%CL | n | $EC_{50}$ | 95% CL | $n_H$ | 95%CL |
| wild-type | 6 | 19.93 | 17.43-22.79 | 1.8 | 1.4-2.1 | 5 | 0.163 | 0.118-0.226 | 1.4 | 0.8-1.9 |
| A309V | 6 | 13.24 | 11.73-14.94 | 1.0 | 0.9-1.1 | 5 | 0.780 | 0.648-0.940 | 1.0 | 0.8-1.2 |
| A309I | 6 | 1.673 | 1.514-1.847 | 2.5 | 2.0-2.9 | 5 | 0.250 | 0.155-0.404 | 1.1 | 0.6-1.6 |
| A309G | 6 | 34.60 | 27.47-43.60 | 0.7 | 0.6-0.8 | 5 | 0.153 | 0.132-0.177 | 1.8 | 1.4-2.2 |
| G315E | 6 | 10.35 | 8.689-12.33 | 1.0 | 0.9-1.2 | 5 | 80.320 | 53.87-119.7 | 0.5 | 0.4-0.6 |

**Table 3**

Levels of resistance to abamectin and the A309V mutation frequencies in field *P. xylostella* populations from China.

| Populations | RF[a] | N[b] | A309V | | | Mutation frequency (%) |
|---|---|---|---|---|---|---|
| | | | Ala/Ala | Ala/Val | Val/Val | |
| Pops. from Southwest China | | | | | | |
| TH13 | 345 | 40 | 35 | 5 | 0 | 6.25 |
| MD13 | 491 | 36 | 36 | 0 | 0 | 0 |
| SH13 | 383 | 36 | 36 | 0 | 0 | 0 |
| TH16 | 92 | 20 | 16 | 4 | 0 | 10 |
| Pops. from Southeast China | | | | | | |
| GZ14 | 49 | 30 | 30 | 0 | 0 | 0 |
| ZC14 | 151 | 30 | 30 | 0 | 0 | 0 |
| SZ14 | 253 | 30 | 30 | 0 | 0 | 0 |
| HZ14 | 162 | 30 | 30 | 0 | 0 | 0 |
| HK15 | 86 | 22 | 22 | 0 | 0 | 0 |
| Pops. from Eastern China | | | | | | |
| NJ14 | 4.7 | 30 | 30 | 0 | 0 | 0 |
| HF14 | 12 | 30 | 30 | 0 | 0 | 0 |
| JN14 | 24 | 30 | 30 | 0 | 0 | 0 |
| KS14 | 3.1 | 30 | 29 | 0 | 1 | 3.33 |
| NJ15 | 14 | 30 | 30 | 0 | 0 | 0 |
| HF15 | 3.3 | 30 | 30 | 0 | 0 | 0 |
| JN15 | 2 | 30 | 30 | 0 | 0 | 0 |
| KS15 | 12 | 30 | 29 | 1 | 0 | 1.67 |

[a] RF (resistance factor) = $LC_{50}$ (resistant strain) ÷ $LC_{50}$ (Roth). Unpublished data.

[b] Number of insects genotyped. A, alanine (Ala); V, valine (Val).

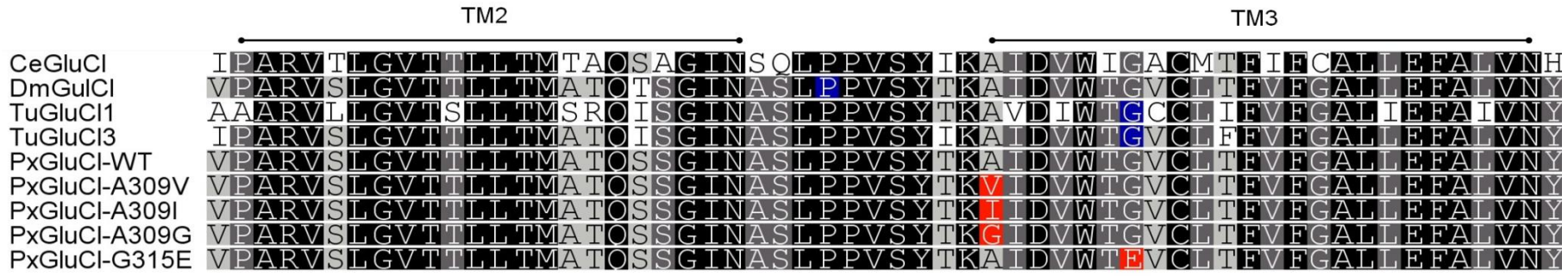


**Fig. 1.** Alignment of the amino acid sequences in transmembrane domain 2 and 3 of glutamate-gated chloride channel genes of *C. elegans* (CeGluCl, GenBank accession code AAA50785.1 ), *D. melanogaster* (DmGluCl, GenBank accession codeU58776.1), *T. urticae* (TuGluCl1, TuGluCl3, GenBank accession code XM_015938823.1 and NP_001310061.1) and *P. xylostella* (PxGluCl-WT, PxGluCl-A309V, PxGluCl-A309I, PxGluCl-A309G, PxGluCl-G315E).Fully conserved resides are shaded in black, while lower similar positions are shaded in grey. The P229S, G314D and G326E mutations in DmGluCl, TuGluCl1 and TuGluCl3, associated with ivermectin/abamectin resistance, are indicated in blue (Kane et al., 2000; Kwon et al., 2010; Dermauw et al., 2012). The A309V mutation in PxGluCl associated with abamectin resistance (Wang et al., 2016b) and the introduced A309I/G and G315E substitutes in this study are indicated in red.

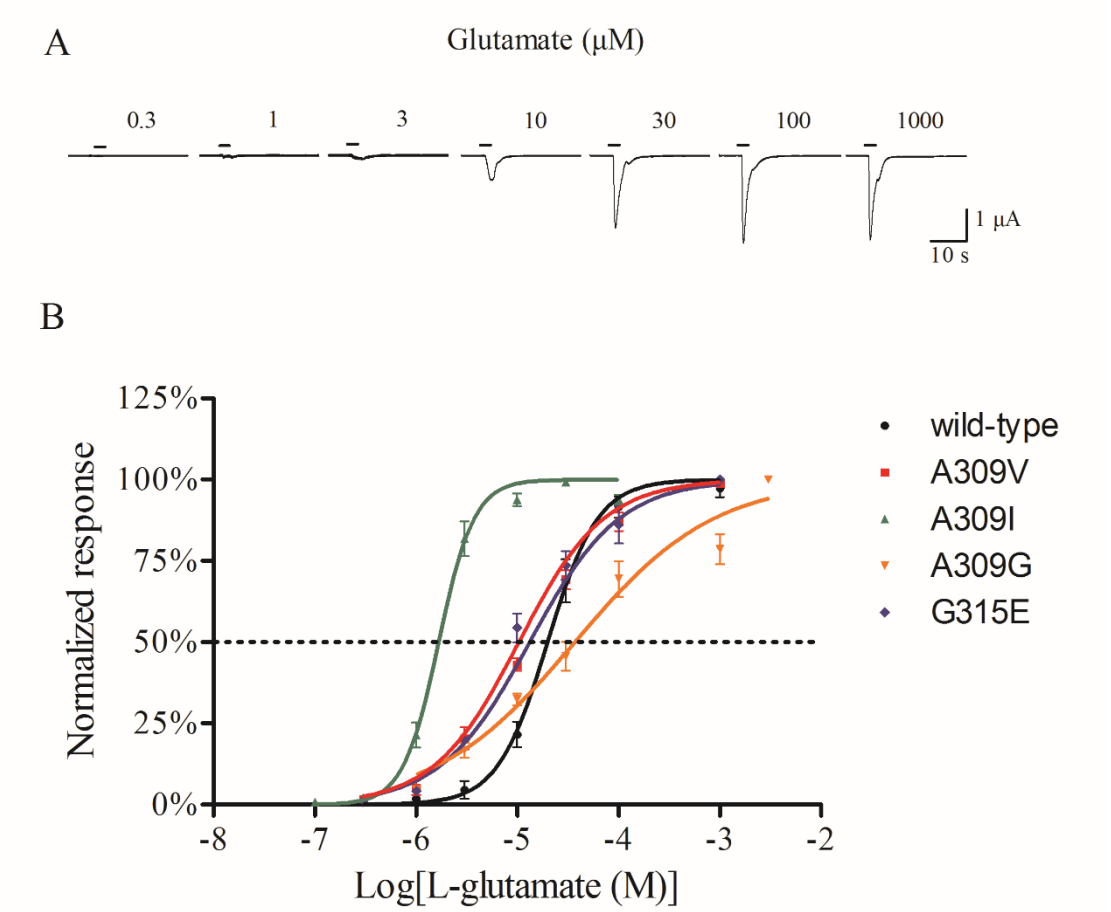


**Fig. 2.** Glutamate responses of wild- and mutant-type homomeric PxGluCls expressed in *Xenopus* oocytes. (A) Traces of electrical responses induced by L-glutamate from the wild-type ion channels. (B) Normalized dose-response curves for glutamate induced currents for oocytes expressing wild-type, A309V, A309I, A309G and G315E mutant channels. The data are means ± SEM (n = 6).

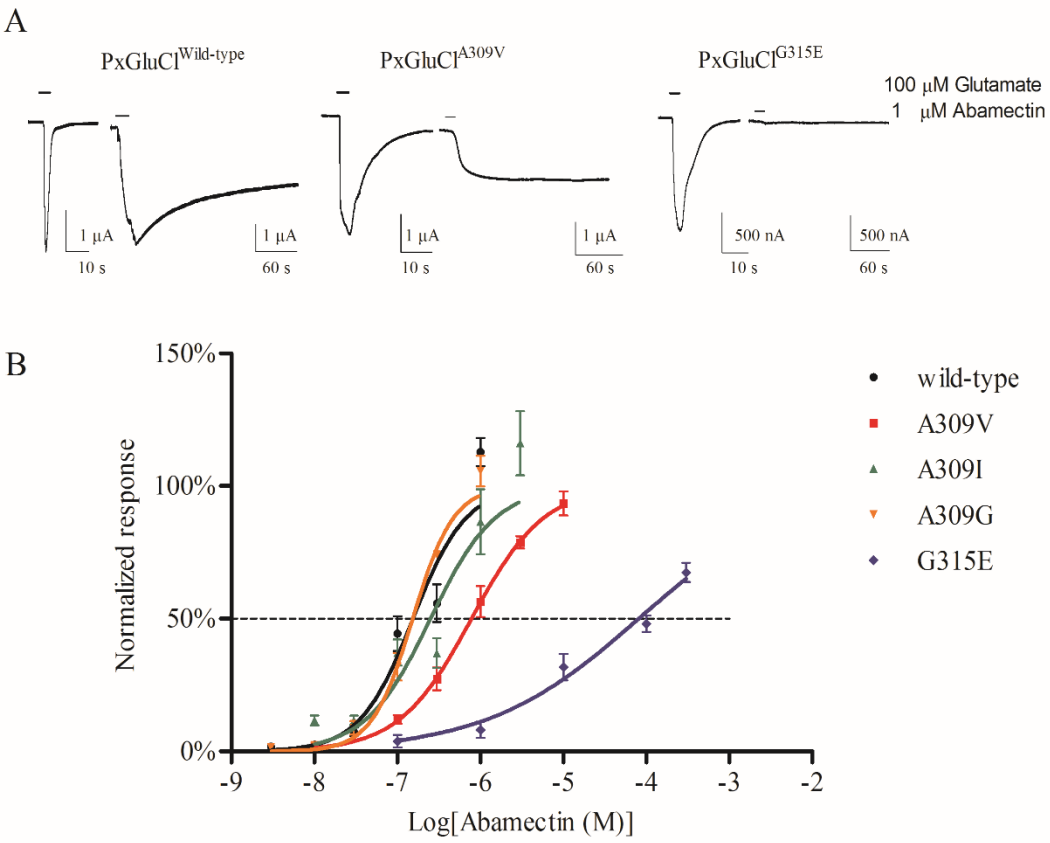


**Fig. 3.** Abamectin responses of wild- and mutant-type homomeric PxGluCls expressed in *Xenopus* oocytes. (A) Examples of electrical responses induced by saturated glutamate (100 μM) and abamectin (1μM) in the wild-type, A309V and G315E mutant ion channels, respectively. (B) Normalized dose-response curves for abamectin induced currents for oocytes expressing wild-type, A309V, A309I, A309G and G315E mutant channels. The data are means ± SEM (n = 5).

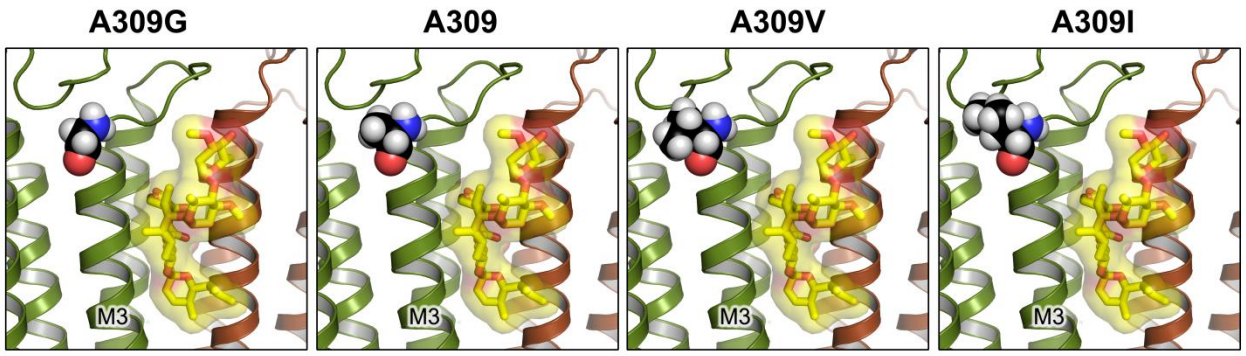


**Fig. 4.** Models of wild-type PxGluCl and A309 mutations. Side view of the transmembrane domain with channel monomers shown as cartoon. The 309 position is shown in black spacefill and abamectin is shown as yellow sticks with a transparent surface.

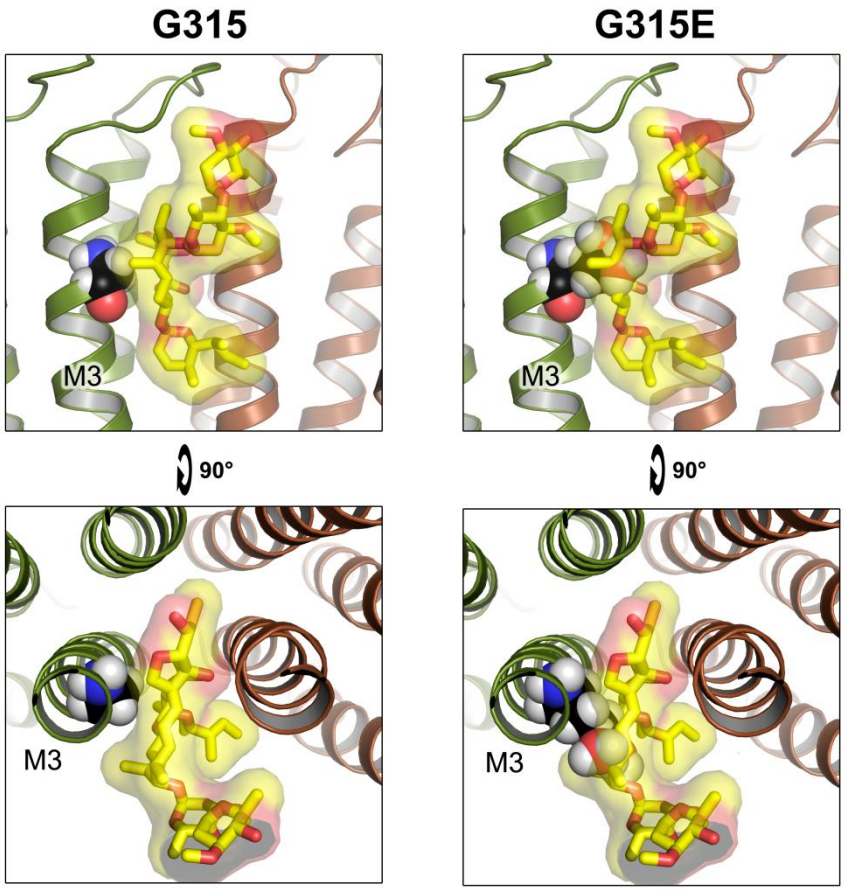


**Fig. 5.** Models of wild-type PxGluCl and the G315 Emutation. Side view and extracellular view of the abamectin binding site with channel monomers shown as cartoon. The 315 position is shown in black spacefill and abamectin is as yellow sticks with a transparent surface.